^{68}Ga-Pentixafor PET/CT Demonstrating In Vivo CXCR4 Receptor Overexpression in Rare Lung Malignancies: Correlation with Histologic and Histochemical Findings

Ankit Watts[1], Baljinder Singh[1], Harmandeep Singh[1], Harneet Kaur[1], Amanjit Bal[2], Mehak Vohra[3], Sunil K. Arora[3], and D. Behera[4]

[1]Department of Nuclear Medicine, Postgraduate Institute of Medical Education and Research, Chandigarh, India; [2]Department of Histopathology, Postgraduate Institute of Medical Education and Research, Chandigarh, India; [3]Department of Immunopathology, Postgraduate Institute of Medical Education and Research, Chandigarh, India; and [4]Department of Pulmonary Medicine, Postgraduate Institute of Medical Education and Research, Chandigarh, India

^{68}Ga-pentixafor PET/CT imaging allows noninvasive assessment of C-X-C chemokine receptor type 4 (CXCR4) expression in various malignancies, but its use in rare lung cancer variants has not been reported. **Methods:** ^{68}Ga-pentixafor PET/CT imaging was performed on 6 patients (3 men, 3 women; mean age, 57.0 ± 16.8 y) with suspected lung masses. Whole-body PET/CT images were acquired 1 h after intravenous injection of 148.0–185.0 MBq of the tracer. PET/CT images were reconstructed and analyzed. The image findings were correlated with histopathologic and quantitative (CXCR4) fluorescence-activated cell sorting analysis. **Results:** Histopathologic diagnosis of hemangioendothelioma, sarcomatoid carcinoma, and hemangiopericytoma was confirmed in 1 patient each. Lung metastasis was diagnosed in the remaining 3 of 6 patients with primary sarcoma (n = 1), renal cell carcinoma (n = 1), and unknown primary (n = 1). Increased uptake in the primary lung mass, with an SUV_{max} of 3.0, 6.34, and 13.0, was noted in the hemangiopericytoma, sarcomatoid carcinoma and hemangioendothelioma cases, respectively. The mean SUV_{max}, mean fluorescence intensity, and percentage of stained cells were highest in hemangioendothelioma. Among 3 patients with lung metastases, the highest SUV_{max}, 9.5, was in the primary sarcoma patient. **Conclusion:** ^{68}Ga-pentixafor selectively targets the in vivo whole-body disease burden of CXCR4 receptors. This approach thus holds promise for developing suitable radiotheranostics for lung cancers expressing these targets.

Key Words: [^{68}Ga]pentixafor; PET/CT imaging; CXCR4 receptors; lung cancer; rare variants; metastasis

J Nucl Med Technol 2022; 50:278–281
DOI: 10.2967/jnmt.122.264141

Despite ever-evolving research and advances in diagnostic and treatment strategies, lung carcinoma remains the most lethal type of cancer worldwide (*1*). The diagnostic work-up in suspected lung tumors involves tissue diagnosis, including histopathology and immunohistochemistry analysis and imaging. A presumptive differentiation between small cell lung cancer (SCLC) and non–small cell lung cancer (NSCLC) can be made on the basis of clinical presentation and radiologic findings (*2*). Functional tumor imaging using ^{18}F-FDG PET/CT offers complementary information by assessing tumor burden and helps in staging (*3*). However, noninvasive PET/CT imaging of receptor expression and the heterogeneity of specific receptors can provide complementary information (*4*).

There is evidence that SCLC and NSCLC display C-X-C chemokine receptor type 4 (CXCR4) overexpression, which is associated with high tumor aggressiveness, metastasis, and recurrence (*5*). CXCR4 expression is analyzed using immunohistochemistry and fluorescence-activated cell sorting (FACS) analysis of biopsy samples (*6*). Noninvasive imaging using high-throughput PET probes targeting CXCR4 receptors may provide important diagnostic or prognostic information on such patients (*7*).

Few studies have described the feasibility of radiolabeling a cyclic pentapeptide (pentixafor) with ^{68}Ga, and the recent use of ^{68}Ga-pentixafor has yielded encouraging preclinical and clinical results for in vivo imaging of CXCR4 expression in solid tumors as well as in hematologic malignancies (*8–10*). The use of ^{68}Ga-pentixafor PET/CT imaging for selective targeting of CXCR4 receptors has made much progress in hematologic malignancies, whereas its role in solid tumors has been seldom reported (*11–13*).

Because there are more than 30 human malignancies known to overexpress CXCR4 receptors, the imaging applications of ^{68}Ga-pentixafor PET/CT for targeting these receptors are fast expanding in other malignancies. It has recently been reported that ^{68}Ga-pentixafor PET/CT shows high tumor uptake in patients with lung cancer (SCLC and NSCLC), glioblastoma multiforme, and multiple myeloma. This tracer exhibited strong affinity and specificity for the in vivo localization and imaging of CXCR4 receptors in these malignancies (*11,14–16*).

In this study, we investigated—for the first time, to our knowledge—the diagnostic utility of ^{68}Ga-pentixafor PET/CT

Received Mar. 22, 2022; revision accepted Apr. 27, 2022.
For correspondence or reprints, contact Baljinder Singh (drbsingh5144@yahoo.com).
Published online May 24, 2022.

imaging in a few cases of rare lung cancer variants and in lung metastasis cases with distant primaries.

MATERIALS AND METHODS

Six patients (3 men, 3 women; mean age, 57.00 ± 16.80 y; range, 33–73 y) with clinically and radiologically suspected lung cancer were recruited prospectively for the study. Written informed consent was obtained from all participants. The protocol was approved by the Institute Ethics Committee as the doctoral thesis of the first author. All patients underwent ^{68}Ga-pentixafor PET/CT, bronchoscopic or PET/CT-guided lung biopsy, routine histopathology, immunohistochemistry, and quantitative CXCR4 receptor analysis by FACS.

^{68}Ga-Pentixafor PET/CT Data Acquisition and Analysis

Briefly, 148.0–185.0 MBq of ^{68}Ga-pentixafor were injected intravenously. Whole-body PET (Discovery; GE Healthcare) and contrast-enhanced CT (using standard CT acquisition parameters) were performed consecutively 1 h after tracer administration. The PET was performed at a rate of 3 min/frame (7–8 frames) from the base of the skull to the proximal thighs. Attenuation-corrected PET images were reconstructed iteratively using ordered-subset expectation maximization. The reconstructed images were projected in 3 planes (cross-sectional, coronal, and sagittal) and used for visual and quantitative (SUV_{max}) analysis.

FACS Analysis

In FACS analysis, the freshly biopsied lung sample was processed, and 5.0 μL of fluorescein isothiocyanate–labeled CD184 (BD Pharmingen) was used to further label the CXCR4-positive tumor cells in the tissue suspension. A flow cytometer (FACS Calibur; BD) was used to analyze the stained and unstained cell population, and the results were expressed as mean fluorescence intensity (MFI) and percentage of CXCR4-positive stained cells.

The ^{68}Ga-pentixafor PET/CT image findings (SUV_{max}) were compared with histopathology and with the quantitative parameters of the FACS assay—that is, the MFI and the percentage of stained cells.

RESULTS

The results of histopathology, FACS, and ^{68}Ga-pentixafor PET are presented in Table 1. High uptake was noted in all lung lesions. In 3 patients (patients 1–3), rare primary lung pathologies were identified. The highest SUV_{max}, 13.04, with the highest corresponding MFI, 682.0, was noted in the patient (patient 2) with histopathologic evidence of hemangioendothelioma (Fig. 1). The SUV_{max} and MFI were 6.34 and 110.5, respectively, in patient 1 (sarcomatoid carcinoma) and 3.0 and 27.90, respectively, in patient 3 (hemangiopericytoma). The corresponding SUV_{max} and MFI were 9.5 and 191.20, respectively, in a case of secondary lung metastasis from sarcoma (patient 4), 6.0 and 62.0, respectively, in a case of renal cell carcinoma (patient 5), and 7.5 and 216.0, respectively, in a case of unknown primary (patient 6). The results of ^{68}Ga-pentixafor PET/CT, FACS, and histopathologic analysis for patient 4 are presented in Figure 2.

Pearson correlation analysis indicated a significant correlation between SUV_{max} and MFI ($r = 0.90$), between SUV_{max} and percentage of stained cells ($r = 0.79$), and between MFI and percentage of stained cells ($r = 0.72$).

DISCUSSION

In the present study, ^{68}Ga-pentixafor PET/CT imaging demonstrated high uptake (SUV_{max}, 13.0; MFI, 682.0) in hemangioendothelioma. The SUV_{max} in the other 2 pathologies—that is, sarcomatoid carcinoma and hemangiopericytoma—varied as a function of MFI. Interestingly, among the 3 cases of lung metastases, the highest SUV_{max}, 9.5 (MFI, 191.0), was seen in the lung metastasis with sarcoma as the primary disease. These findings presented a positive correlation ($r = 0.90$) between ^{68}Ga-pentixafor uptake and CXCR4 receptor expression and density, which in turn indicated the high specificity of the tracer for these receptors. Likewise, SUV_{max} also correlated ($r = 0.79$) with the percentage of stained cells.

To our knowledge, we were the first to report the normal biodistribution of ^{68}Ga-pentixafor in a healthy volunteer; the highest SUV_{mean} and SUV_{max} were in the urinary bladder (146.0 and 239.0, respectively) and spleen (6.80 and 10.10, respectively), followed by the kidneys (4.99 and 20.55, respectively) (*17*). Variable physiologic uptake of ^{68}Ga-pentixafor was seen in the spleen in different imaging studies and was found to have an association with stage of disease and clinical outcome, as reported in a study on 145 solid-tumor patients (*18*). A positive correlation was found between ^{68}Ga-pentixafor splenic uptake and platelet or leukocyte counts in lung cancer and neuroendocrine tumors, suggesting that splenic uptake might play a role in systemic immunity or inflammation (*18*).

TABLE 1
Findings in 6 Patients with Rare Lung Tumors and Metastatic Lung Disease

Patient no.	Age (y)	Sex	Histopathology	^{68}Ga-pentixafor PET SUV_{max}	FACS analysis	
					MFI	CXCR-positive tumor cells (%)
1	73	F	Sarcomatoid carcinoma (primary tumor)	6.34	110.50	2.70
2	33	F	Hemangioendothelioma (primary tumor)	13.0	682.0	73.60
3	68	M	Hemangiopericytoma (primary tumor)	3.0	27.90	2.50
4	70	F	Lung metastasis (primary sarcoma)	9.5	191.20	45.2
5	40	M	Lung metastasis (primary renal cell carcinoma)	6.0	62.0	47.0
6	58	M	Lung metastasis (unknown primary)	7.5	216.6	59.2

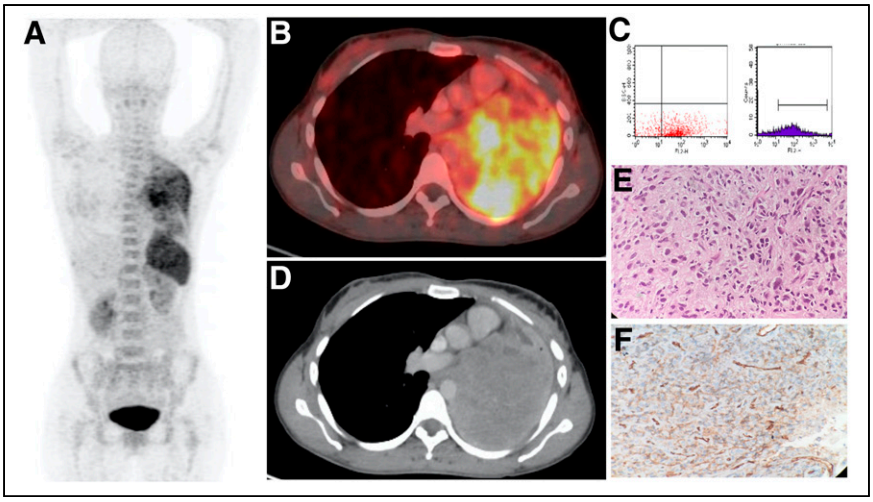

FIGURE 1. A 73-y-old woman (patient 2) with primary lung hemangioendothelioma. (A, B, and D) ^{68}Ga-pentixafor PET/CT maximum-intensity projection (A) and cross-sectional PET/CT image (B) showing increased uptake (SUV_{max}, 13.0), with corresponding CT image (D). (C, E, and F) FACS analysis using CD184-PE showing stained CXCR4-positive tumor cells in scatterplots (C), photomicrograph with histopathologic disease evidence showing epithelioid tumor cells (hematoxylin and eosin, ×40) (E) and immunohistochemistry staining with CD31 showing diffuse membranous positivity (F).

We previously reported that uptake of ^{68}Ga-pentixafor in SCLC patients was higher than in NCSLC and other lung cancer variants and that the uptake varied as a function of CXCR4 receptor density (*11,14*). However, the pattern of uptake and the in vivo evidence of CXCR4 expression in rare lung malignancies have not been studied before.

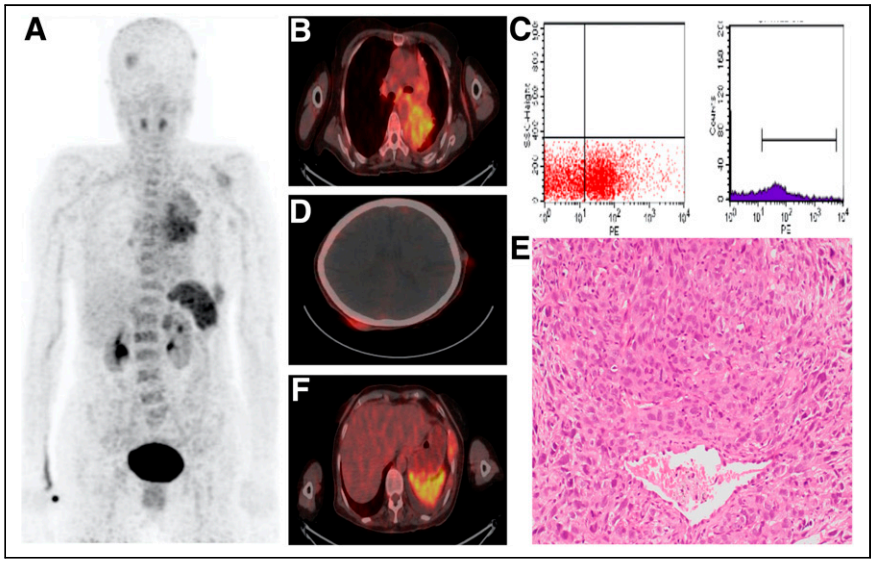

FIGURE 2. A 70-y-old woman (patient 4) with secondary lung cancer disease. (A) ^{68}Ga-pentixafor PET/CT maximum-intensity projection showing increased uptake in lung and in multiple sarcomatoid lesions. (B, D, and F) Cross-sectional PET/CT image showing increased (SUV_{max}, 9.5) uptake in metastatic lung lesion (B), in posterior subcutaneous lesions and left lateral aspect of scalp (SUV_{max}, 4.6) (D), and in lytic expansile lesion with soft-tissue component involving lateral aspect of fifth rib (SUV_{max}, 5.4) (F). (C) FACS analysis using CD184-PE showing stained CXCR4-positive tumor cells in scatterplots. (E) Photomicrograph with histopathologic disease evidence (hematoxylin and eosin, ×40).

^{68}Ga-pentixafor PET tracer was shown to have excellent affinity for CXCR4 receptors in preclinical and clinical studies (*19,20*). According to the available literature, noninvasive imaging of CXCR4 expression in SCLC is feasible, and ^{68}Ga-pentixafor as a novel PET tracer might serve as a readout for confirming the CXCR4 expression (*20*). Watts et al. reported that ^{68}Ga-pentixafor uptake denoting CXCR4 expression is higher in SCLC than NSCLC patients (*11,14*). Evaluation of CXCR4 expression is a prerequisite for potential CXCR4-directed radiotherapies and chemotherapies in lung cancer and especially in SCLC, which has higher CXCR4 expression compared with all other variants of lung cancer.

The reports on CXCR4 expression in rare lung tumors included in this study are not available. However, the role of overexpression of CXCR4 receptors in tumor growth and progression in sarcoma and renal cell carcinoma primaries and in metastasis to lungs has been demonstrated (*21,22*). ^{68}Ga-pentixafor PET imaging may thus be expanded beyond SCLC and NSCLC to unravel the CXCR4 receptor density and to understand the process of metastatic spread and the intra- or interindividual heterogeneity of these tumors (*23*). In a recent study, an urgent clinical need to develop novel therapeutics for devastating NSCLC disease targeting the CXCR4/CXCL12 axis has been advocated (*24*). The study has further stressed that this is the time to move forward and attempt to incorporate CXCR4 inhibitors into novel immune-based therapeutic protocols for lung cancer.

CONCLUSION

^{68}Ga-pentixafor selectively targets and accurately maps the in vivo whole-body disease burden of CXCR4 receptors, a task that is not possible by tissue sampling methods. This technique thus holds great promise for translating this approach by labeling the vector with α- or β-emitters to a therapeutic scenario in such aggressive lung cancer variants having limited treatment options.

DISCLOSURE

Baljinder Singh of the Department of Nuclear Medicine received extramural research funding from the

Department of Science and Technology under the DST-FIST program (grant SR/FST/LSI-548/2012) for the purchase of the automated chemistry module and other chemicals and peptides. No other potential conflict of interest relevant to this article was reported.

KEY POINTS

QUESTION: Can the in vivo expression of CXCR4 receptors be shown in rare lung cancers noninvasively by ^{68}Ga-pentixafor PET/CT?

PERTINENT FINDINGS: ^{68}Ga-pentixafor PET/CT detected the presence of CXCR4 receptors in rare lung cancers and metastases. The uptake varied as a function of receptor density, showing high specificity for in vivo imaging of CXCR4 receptor disease burden in lung cancers.

IMPLICATIONS FOR PATIENT CARE: This technique holds great promise for translating this approach by labeling the vector with α- or β-emitters for therapeutic applications in aggressive lung cancer variants having limited treatment options.

REFERENCES

1. Barta JA, Powell CA, Wisnivesky JP. Global epidemiology of lung cancer. *Ann Glob Health.* 2019;85:8.
2. Silvestri GA, Gonzalez AV, Jantz MA, et al. Methods for staging non-small cell lung cancer: diagnosis and management of lung cancer, 3rd ed: American College of Chest Physicians evidence-based clinical practice guidelines. *Chest.* 2013; 143(suppl):e211S–e250S.
3. Kandathil A, Kay FU, Butt YM, Wachsmann JW, Subramaniam RM. Role of FDG PET/CT in the eighth edition of TNM staging of non-small cell lung cancer. *Radiographics.* 2018;38:2134–2149.
4. George GP, Pisaneschi F, Nguyen QD, Aboagye EO. Positron emission tomographic imaging of CXCR4 in cancer: challenges and promises. *Mol Imaging.* 2014;13:10.2310/7290.2014.00041.
5. Domanska UM, Kruizinga RC, Nagengast WB, et al. A review on CXCR4/CXCL12 axis in oncology: no place to hide. *Eur J Cancer.* 2013;49:219–230.
6. Stankovic B, Bjørhovde HAK, Skarshaug R, et al. Immune cell composition in human non-small cell lung cancer. *Front Immunol.* 2019;9:3101.
7. Demmer O, Gourni E, Schumacher U, Kessler H, Wester HJ. PET imaging of CXCR4 receptors in cancer by a new optimized ligand. *ChemMedChem.* 2011;6: 1789–1791.
8. Shekhawat AS, Singh B, Malhotra P, et al. Imaging CXCR4 receptors expression for staging multiple myeloma by using 68Ga-Pentixafor PET/CT: comparison with 18F-FDG PET/CT. *Br J Radiol.* 2022;95:20211272.
9. Vag T, Gerngross C, Herhaus P, et al. First experience with chemokine receptor CXCR4-targeted PET imaging of patients with solid cancers. *J Nucl Med.* 2016; 57:741–746.
10. Lapa C, Herrmann K, Schirbel A, et al. CXCR4-directed endoradiotherapy induces high response rates in extramedullary relapsed multiple myeloma. *Theranostics.* 2017;7:1589–1597.
11. Watts A, Singh B, Basher R, et al. ^{68}Ga-pentixafor PET/CT demonstrating higher CXCR4 density in small cell lung carcinoma than in non-small cell variant. *Eur J Nucl Med Mol Imaging.* 2017;44:909–910.
12. Wald O. CXCR4 based therapeutics for non-small cell lung cancer (NSCLC). *J Clin Med.* 2018;7:303.
13. Herrmann K, Schottelius M, Lapa C, et al. First-in-human experience of CXCR4-directed endoradiotherapy with ^{177}Lu- and ^{90}Y-labeled pentixather in advanced-stage multiple myeloma with extensive intra- and extramedullary disease. *J Nucl Med.* 2016;57:248–251.
14. Watts A, Singh B, Dhanota N, et al. In vivo imaging and quantification of CXCR4 expression in lung cancer subtypes using ^{68}Ga-pentixafor PET/CT and flow cytometry analysis: a single center and first Asian experience [abstract]. *J Nucl Med.* 2019;60(suppl 1):84.
15. Watts A, Arora D, Kumar N, et al. ^{68}Ga-pentixafor PET/CT offers high contrast image for the detection of CXCR4 expression in recurrent glioma [abstract]. *J Nucl Med.* 2019;60(suppl 1):491
16. Singh B, Shekhawat A, Malhotra P. Comparison of ^{68}Ga-pentixafor PET/CT versus ^{18}F-FDG PET/CT in staging of multiple myeloma [abstract]. *J Nucl Med.* 2020;61(suppl 1):171.
17. Watts A, Chutani S, Arora D, et al. Automated radiosynthesis, quality control, and biodistribution of Ga-68 pentixafor: first Indian experience. *Indian J Nucl Med.* 2021;36:237–244.
18. Lewis R, Habringer S, Kircher M, et al. Investigation of spleen CXCR4 expression by [^{68}Ga]pentixafor PET in a cohort of 145 solid cancer patients. *EJNMMI Res.* 2021;11:77.
19. Knight JC, Wuest FR. Nuclear (PET/SPECT) and optical imaging probes targeting the CXCR4 chemokine receptor. *MedChemComm.* 2012;3:1039–1053.
20. Lapa C, Lückerath K, Rudelius M, et al. [^{68}Ga]pentixafor-PET/CT for imaging of chemokine receptor 4 expression in small cell lung cancer: initial experience. *Oncotarget.* 2016;7:9288–9295.
21. Zhu Y, Tang L, Zhao S, et al. CXCR4-mediated osteosarcoma growth and pulmonary metastasis is suppressed by microRNA-613. *Cancer Sci.* 2018;109: 2412–2422.
22. Floranović MP, Veličković LJ. Effect of CXCL12 and its receptors on unpredictable renal cell carcinoma. *Clin Genitourin Cancer.* 2020;18:e337–e342.
23. Buck AK, Stolzenburg A, Hänscheid H, et al. Chemokine receptor-directed imaging and therapy. *Methods.* 2017;130:63–71.
24. Osl T, Schmidt A, Schwaiger M, Schottelius M, Wester HJ. A new class of PentixaFor- and PentixaTher-based theranostic agents with enhanced CXCR4-targeting efficiency. *Theranostics.* 2020;10:8264–8280.